Atomic Layer Deposition of Ferroelectric and Threshold Switching Materials for Next Generation Nonvolatile Memory

Karl Littau, Stephen L. Weeks, Ashish Pal, Vijay Narasimhan, Greg Nowling, Michael Bowes, Sergey V. Barabash, Dipankar Pramanik, and Tony Chiang

Who We Are:
Trusted Partner For Materials Innovation

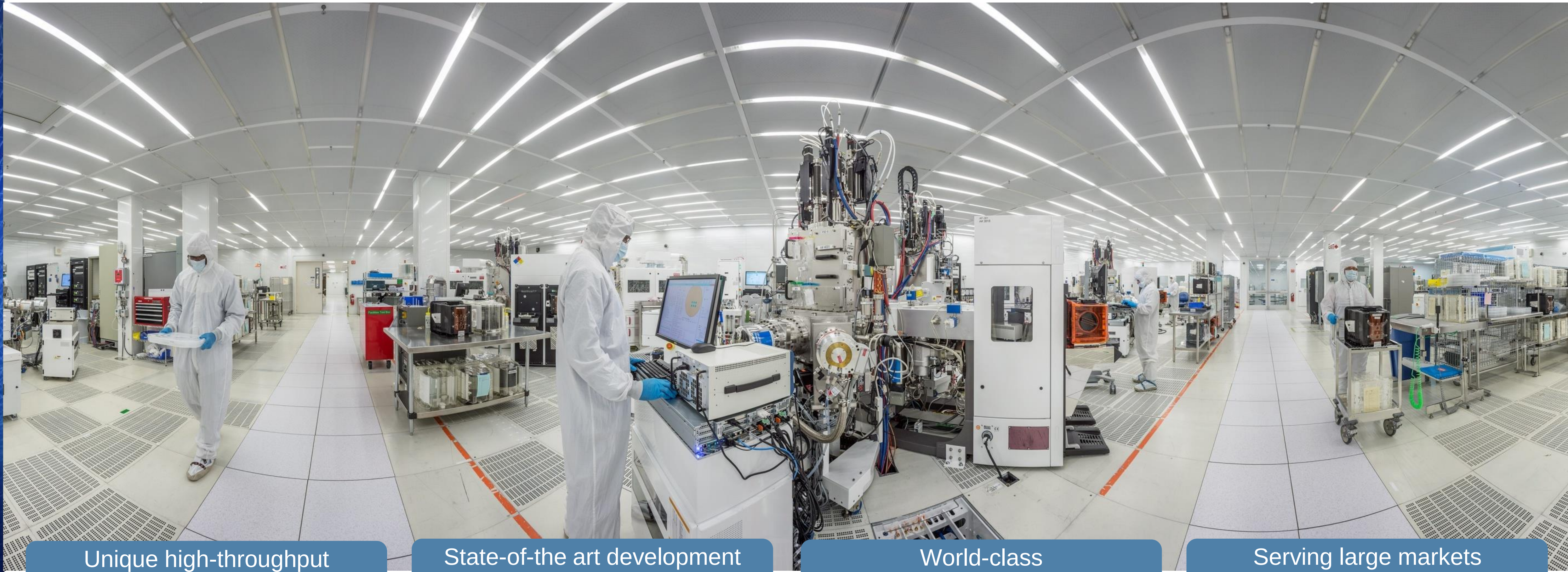

- Unique high-throughput experimentation platform
- State-of-the art development facility and characterization
- World-class interdisciplinary team
- Serving large markets where new materials are key

Fast Facts

Founded:	Intermolecular:	IPO:
2004	HQ in San Jose, CA, USA	2011 (NASDAQ:IMI)

50,000 sq. ft. High Throughput Materials Experimentation Facility

Materials Are at the Core of Innovation in the 21st Century

- Weight
- Space
- Flexibility

- Temperature
- Energy Efficiency
- Smart Buildings

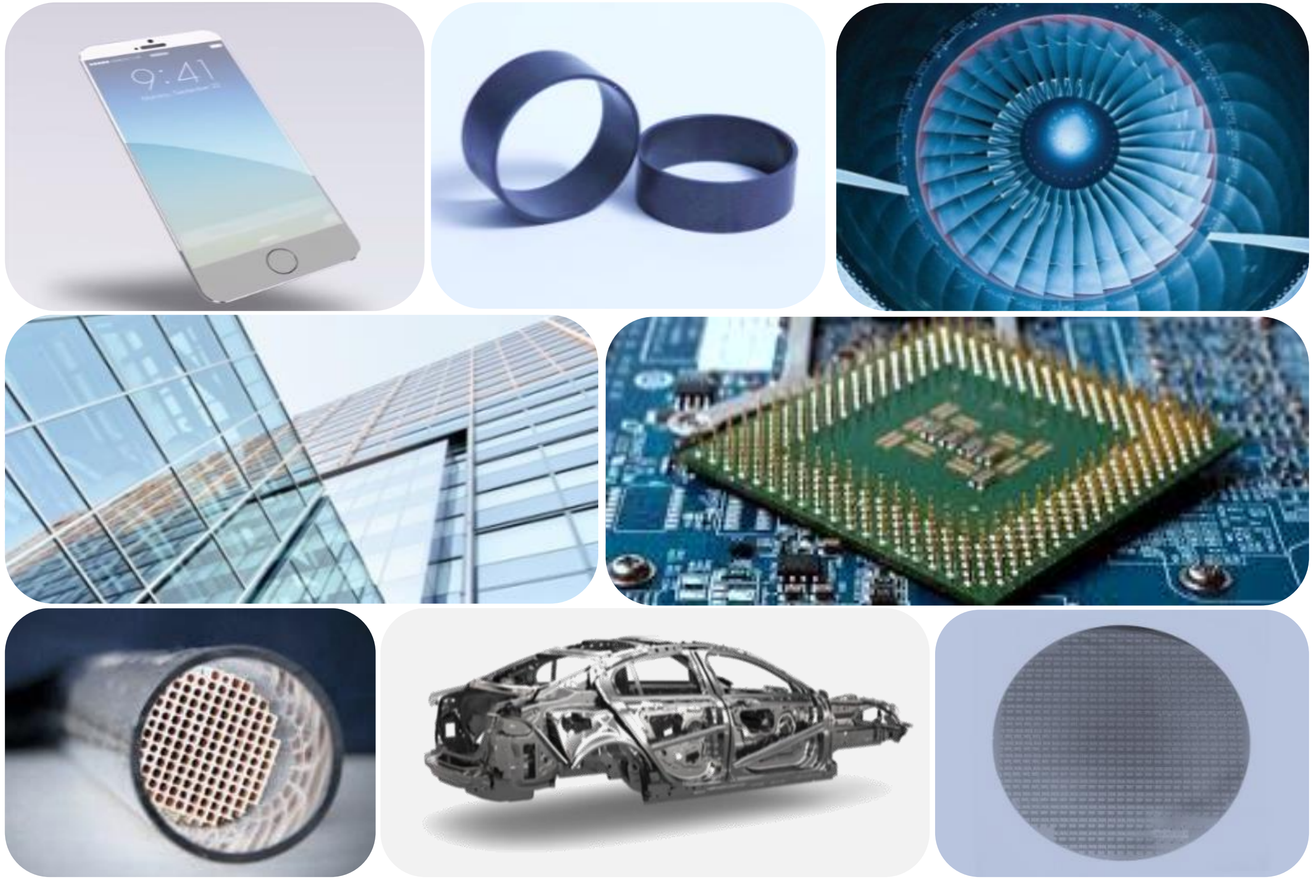

- Heat Management
- Lightweight
- Energy Efficiency

- Performance
- Power
- Cost
- Scaling

- Lightweight
- Energy Efficiency

The Materials Innovation Problem

INTERMOLECULAR

Materials innovation is complex, costly and slow

- Empirical approach needed
- Long learning cycle times
- Manufacturing environment is adverse to change
- Many options, one experiment at a time
- Limited R&D infrastructure for experimentation
- Risk management of new materials

Discovery and Innovation Process

Results

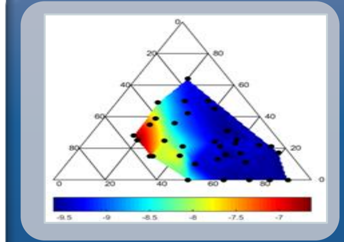

Mapping Materials Space

- Search application specific novel materials
- Composition, mechanical, electrical, optical characterization

Best candidates for exploration

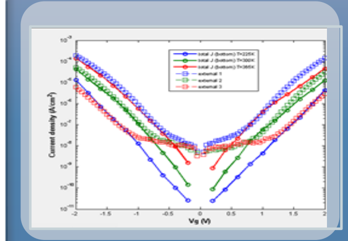

Deep Understanding of Options

- Characterization with application specific tests
- Develop and provide empirical models

Best candidates for applications

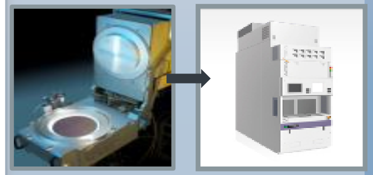

Insertion into Manufacturing

- Application specific multi-layers
- Early process scale-up and validation

Manufacturing compatibility

Integrated Cluster Platform with ALD and PVD

Platform Highlights

Intermolecular designed and built an advanced R&D platform for thin film deposition, enabling rapid exploration of complex materials

- Cluster platform to enable in-situ processing
- A-30 ALD (Atomic Layer Deposition) systems enable full-wafer or quadrant-isolated depositions
- P-30 PVD (Physical Vapor Deposition) systems enable gradient or site-isolated depositions

Example Cluster Configurations

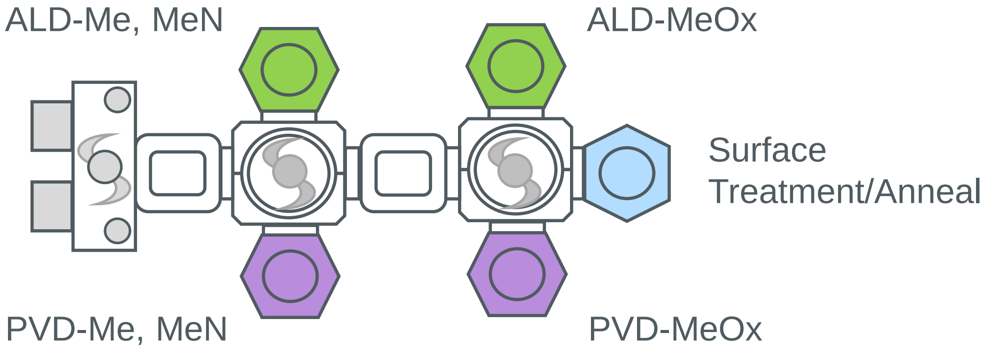

PVD Site-Isolated Deposition

P-30 PVD

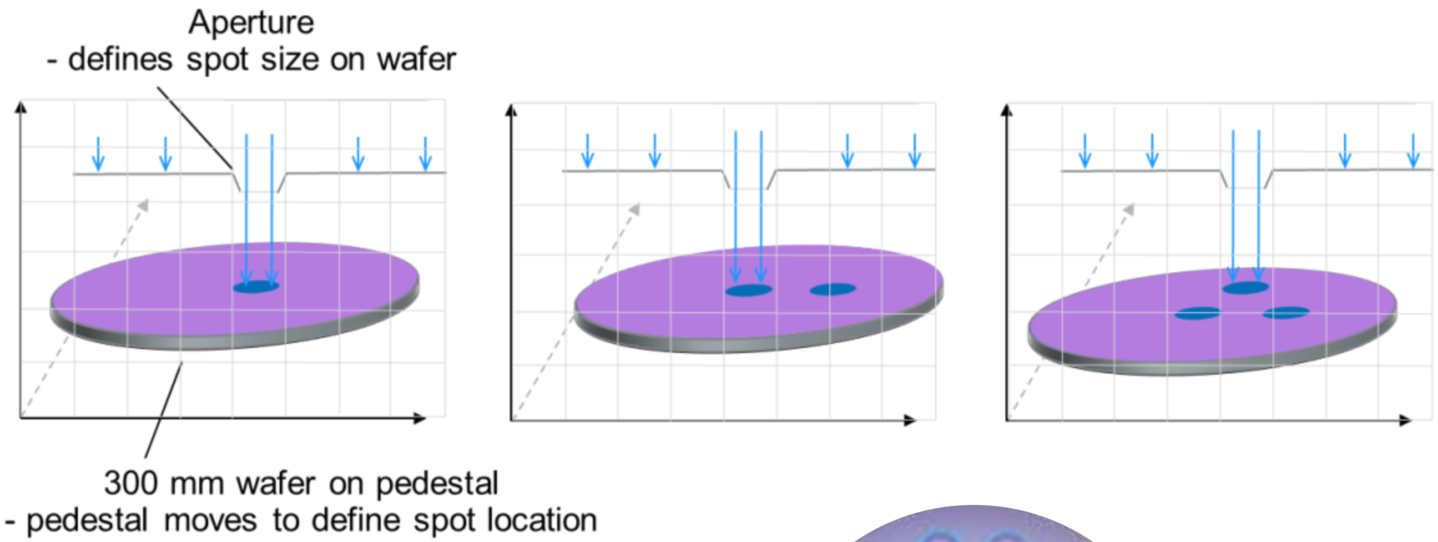

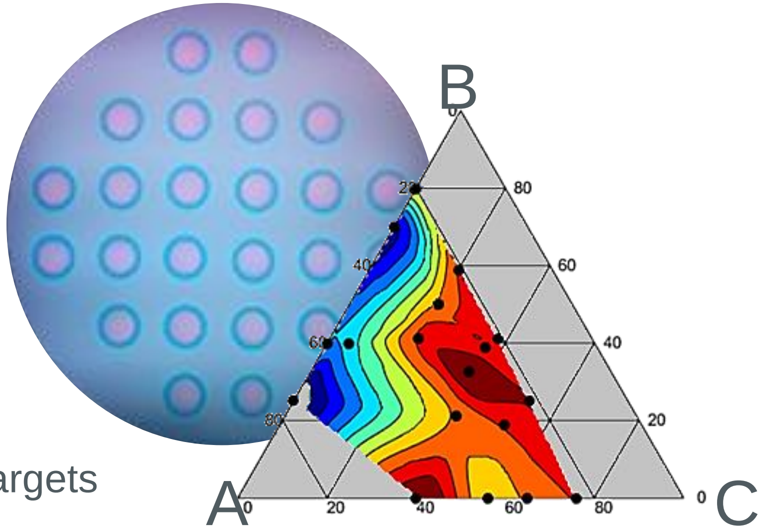

Example for a Ternary Material

Each site is an independent experiment

- Each layer can be deposited by 1 to 4 sputter sources
- Multiple layers can be deposited at one site
- Aperture: defines area where material is deposited; there is no intermixing of areas
- Shutters for Aperture and Target: prevents cross-contamination between layers & targets
- Recipe: includes target cleaning & conditioning before each deposition

A-30 Quadrant-based ALD Chamber

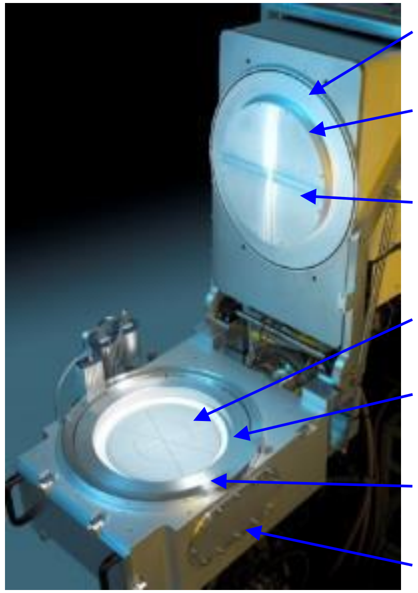

- Full wafer processing
- Independently controlled ALD in 4 quadrants of a single substrate
  - Non-contact gas isolation
  - Separate precursor & reactant delivery lines
  - Low vapor solid, liquid, and or DLI precursors
  - Axi-symmetric, segmented flow

Full Wafer

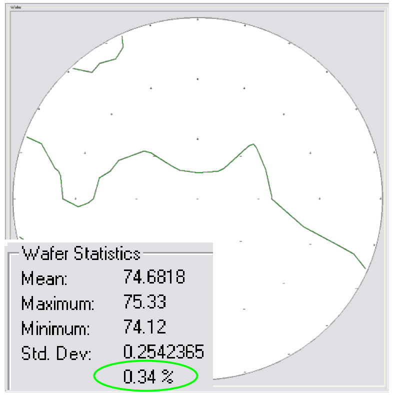

Quadrant-Isolated
Thickness Variation

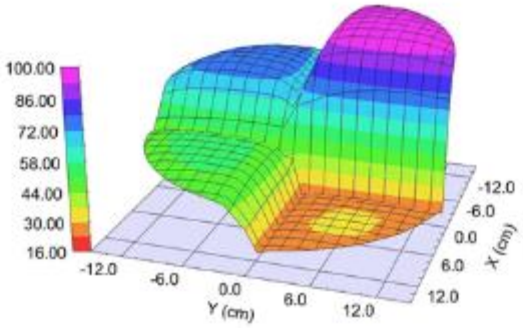

Quadrant-Isolated
Composition Variation

Region	Zr:Hf Cycles	Thickness (A)	%Hf
Q1	5:1	83.3	22%
Q2	6:1	83.0	19%
Q3	7:1	79.4	17%
Q4	8:1	80.7	15%

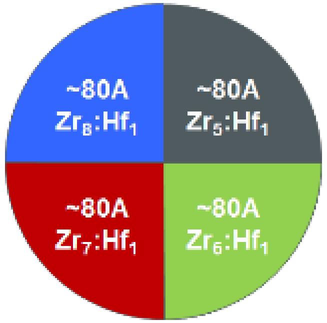

Combi ALD: Model → Design → Implementation

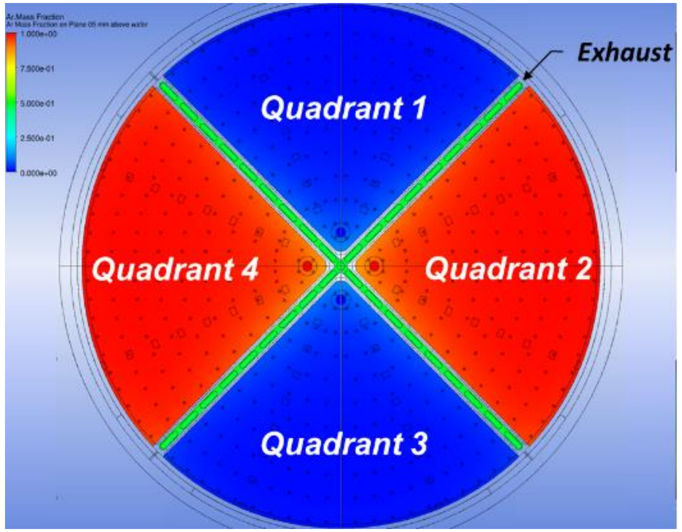

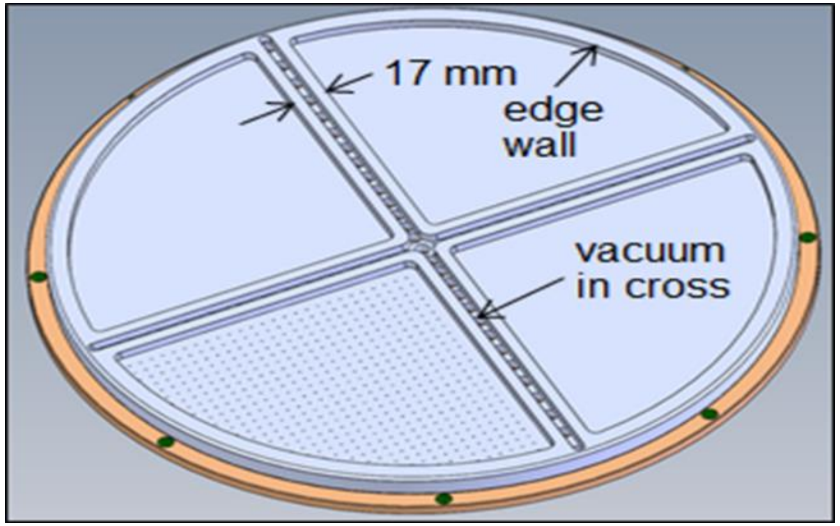

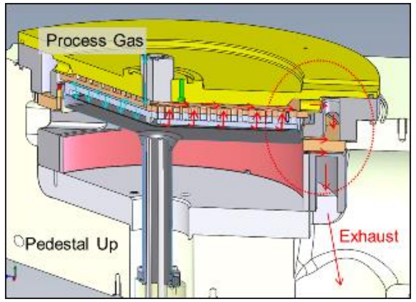

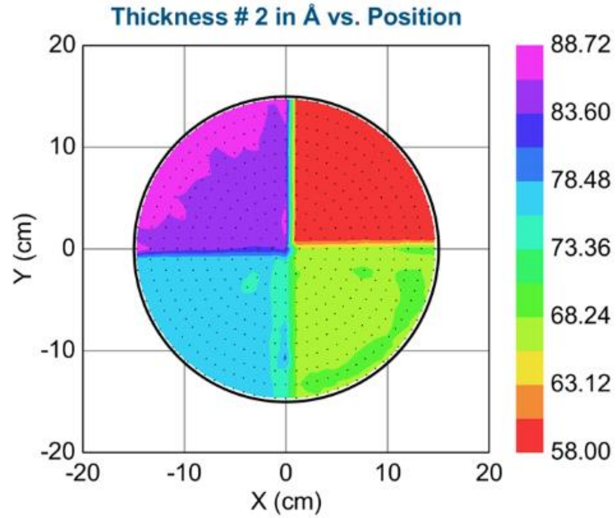

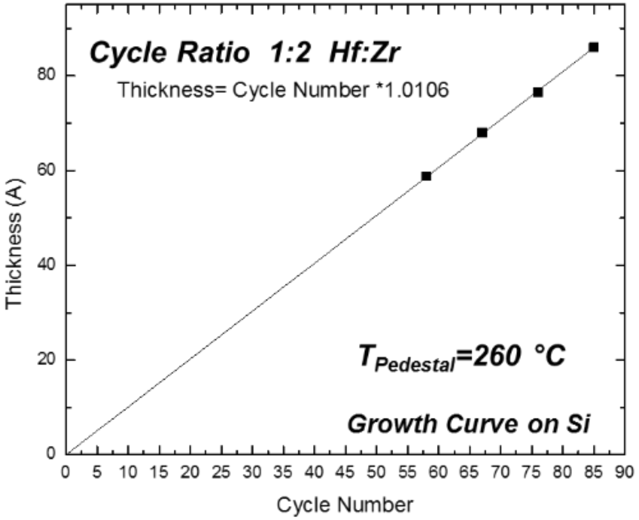

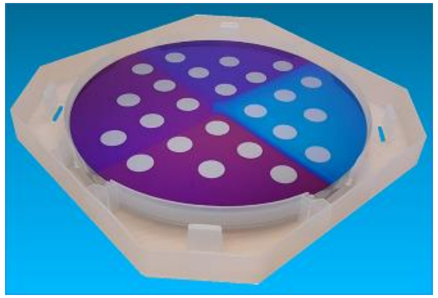

Use Case: Hf/ZrO$_2$ Blended Solid Solution

G. Nowling, et al., “Non-contact, Site-addressable ALD for Rapid Development of Advanced Thin Film Stacks”, ALD 2016 Ireland (2017)

FE Materials

FE Materials: Applications

1T Capacitor-less DRAM

Voltage pulse to the gate affects polarity of FE material which determines whether drain current, I_D, is on (“1” state) or off (“0” state)

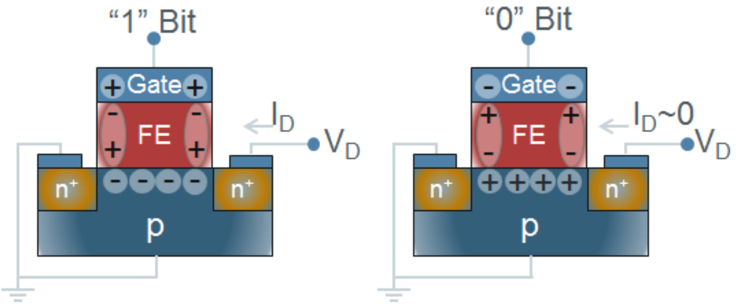

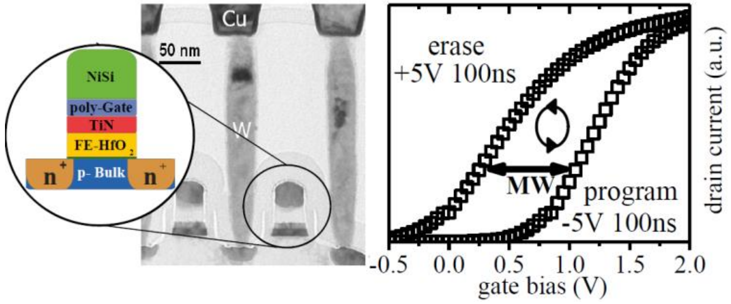

J. Muller et al., VLSI Technology 2012

FTJ-based 3D NVM

Barrier height is modulated by a change in polarization, inducing a current switch

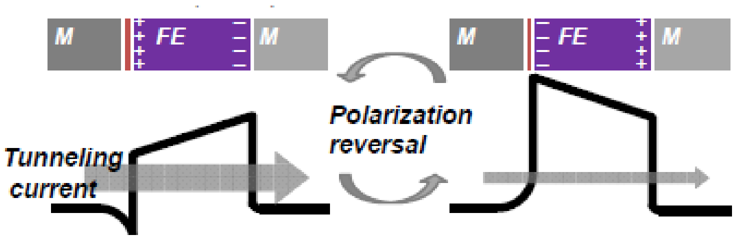

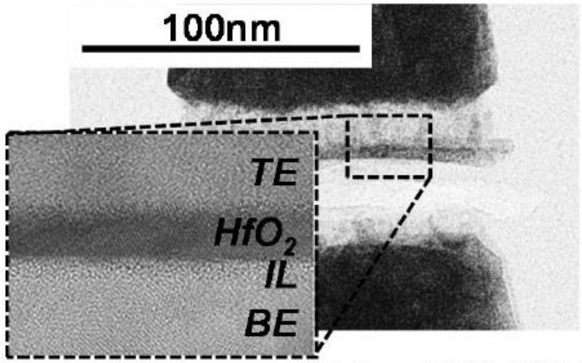

Fig.4 TEM images of fabricated HfO_2 FTJ device.

Fujii et. al., Toshiba, 2016 Symposium on VLSI Technology Digest of Technical Papers

Negative Capacitance FET for Logic

Ferroelectric layer in series with gate dielectric enables negative capacitance resulting in higher subthreshold slope for low power operation

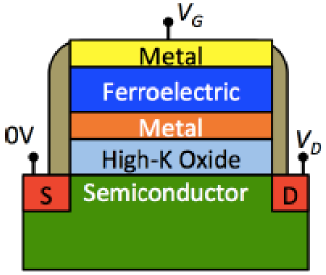

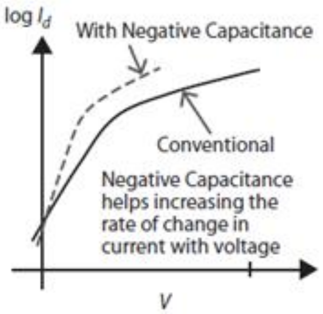

Ref. Salahuddin et. al

FE Materials: Workflow

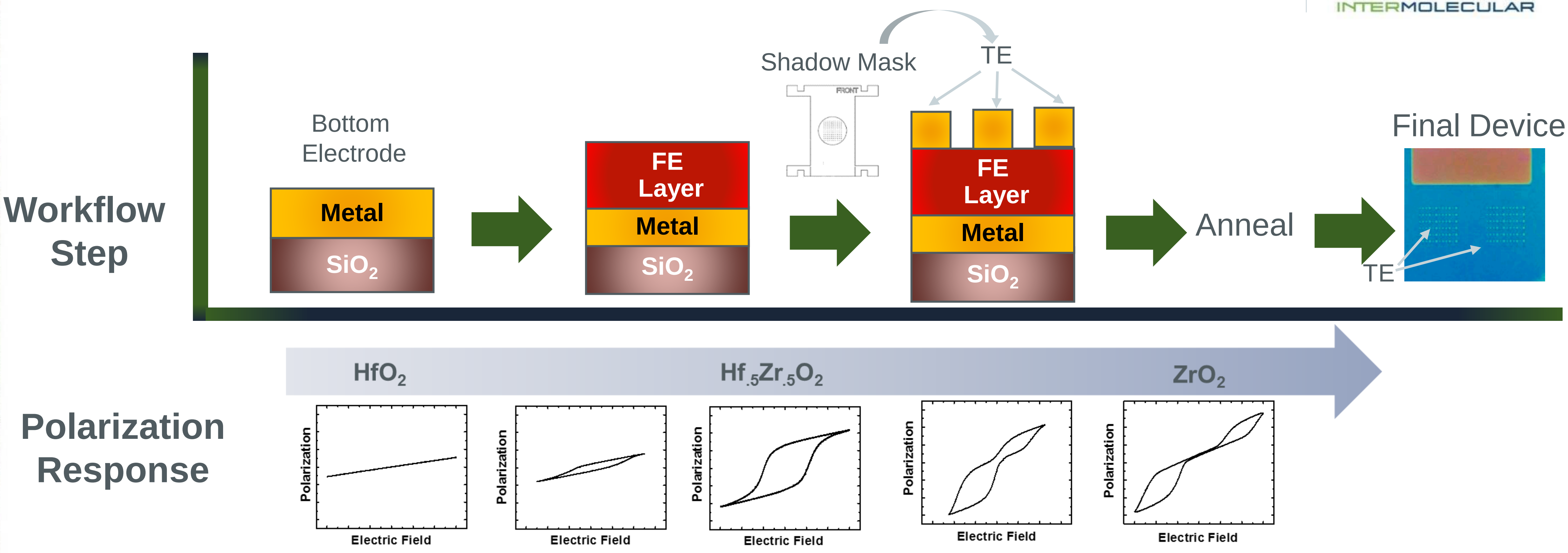

- PVD top and bottom electrodes (optionally ALD).
- 2 Component dielectric (All ALD).
  - Unit films: ZrO_2, HfO_2
- Materials characterization.
- Dielectric and ferroelectric polarization response.

FE HfO_2/ZrO_2 Nanolaminates

Improved FE Response Beyond $HfZrO_2$ By Modulating Layer Thickness

High Q-space XRR (SLAC)

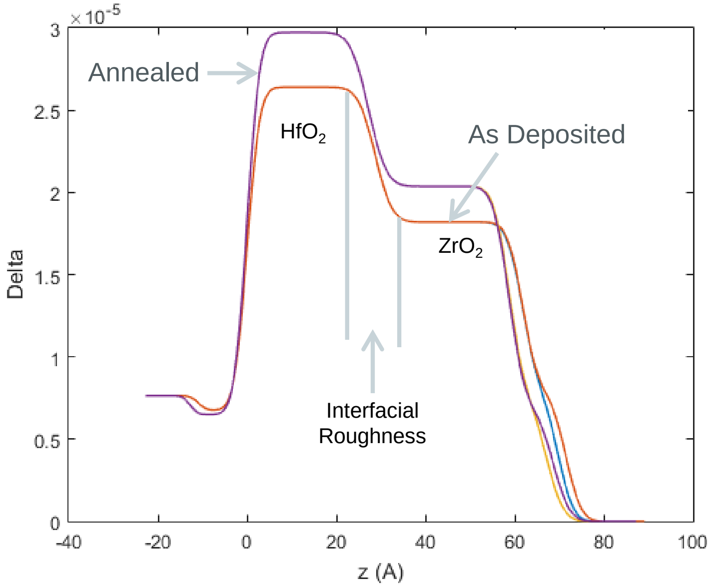

- Synchrotron XRR study confirms no intermixing over larger length scale
    - 3Å interfacial roughness between HfO_2/ZrO_2
    - Maintained after annealing
    - Less than the lattice parameters for tetragonal and orthorhombic HfO_2/ZrO_2

HRTEM: Distinct Layers Maintained To 1nm Layer

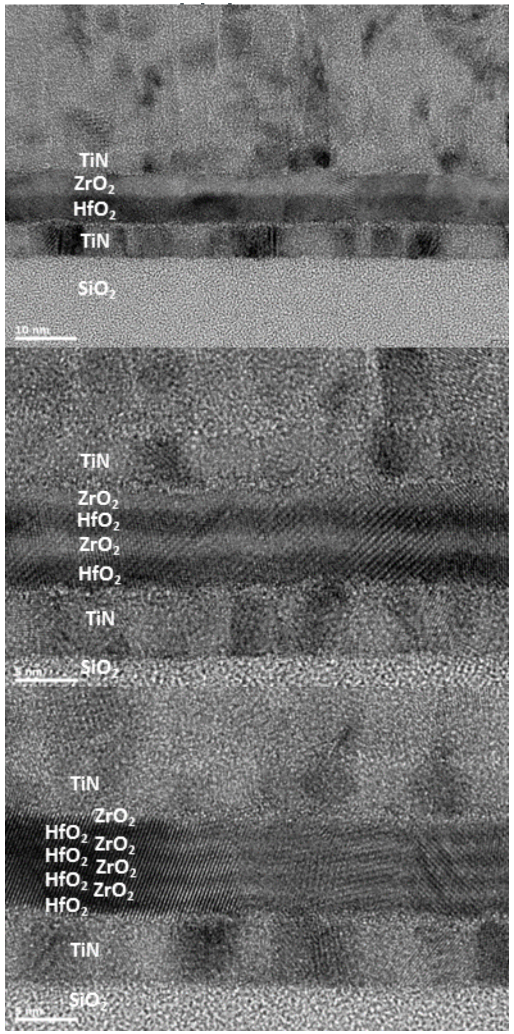

Device Results (After Field Cycling)

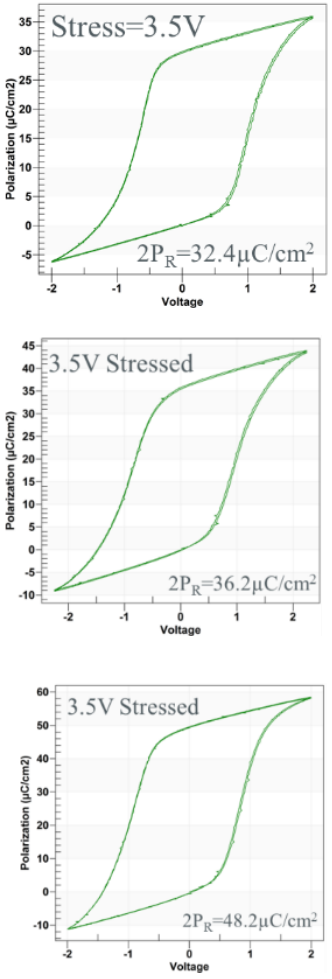

Comparison To Solid Solution

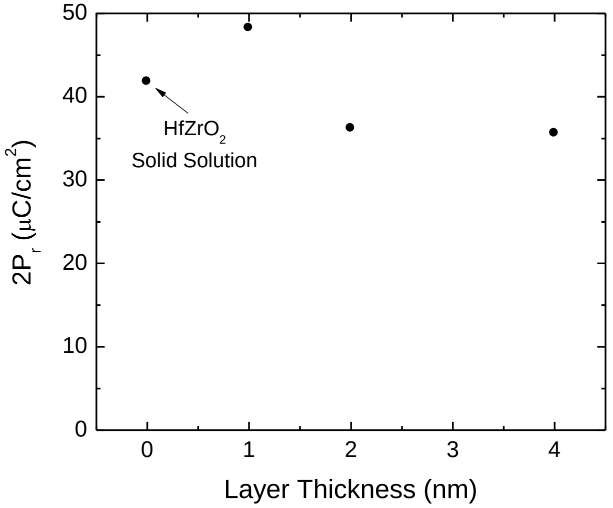

- Modulation of layer thickness can enable nanolaminate ferroelectric performance enhancement over $HfZrO_2$

In conjunction with Advanced Light Source at Stanford Linear Accelerator Center. Lead Scientist Apurva Mehta, Trevor Petach, Ryan Davis, Fang Ren

IMI Results: Undoped FE HfO_2

Process Flow

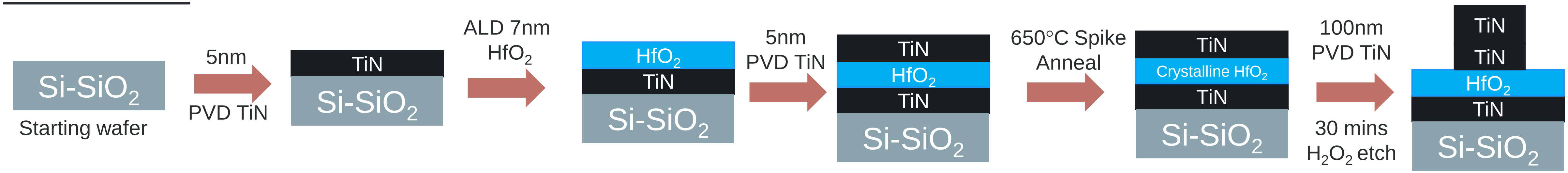

X-Ray Diffraction

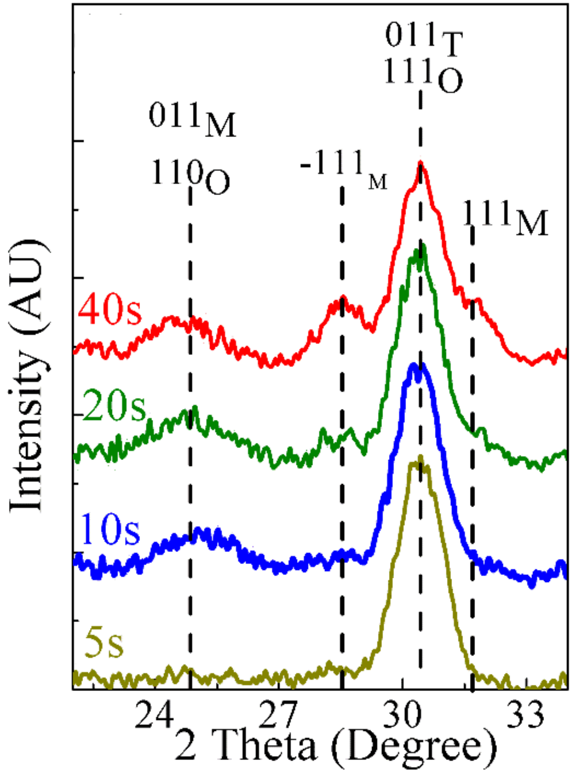

Dielectric Constant

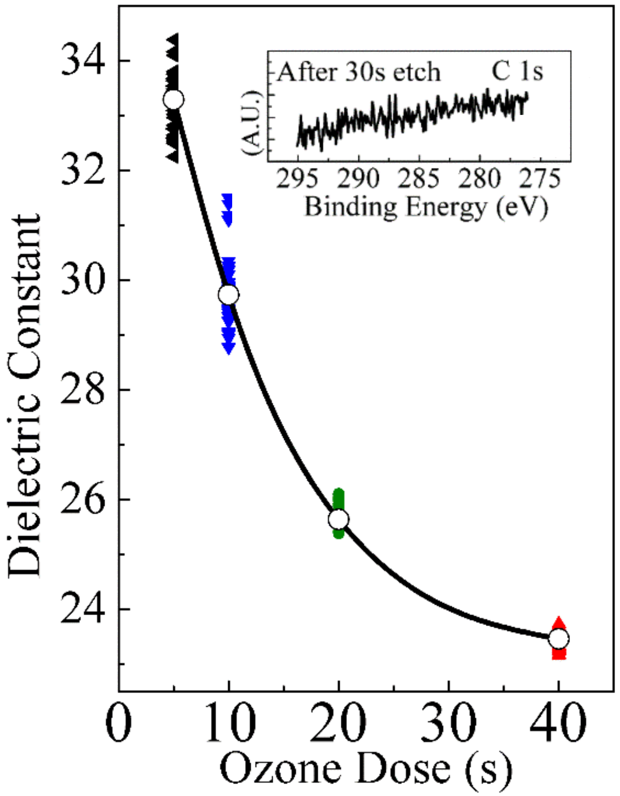

Lower O_3 Dose ⇒

- Lower monoclinic phase
- Higher tetragonal phase
- Higher dielectric constant

A. Pal, et al., "Enhancing Ferroelectricity in Dopant-Free Hafnium Oxide", Applied Physics Letters 110, 022903 (2017)

IMI Results: Undoped FE HfO_2

INTERMOLECULAR

Leakage & Vacancy

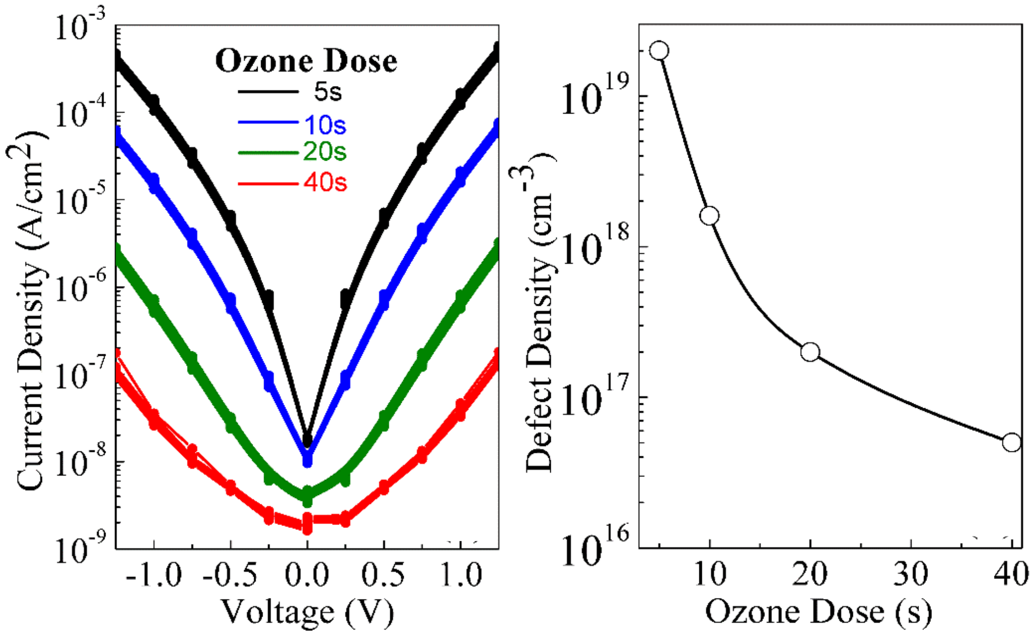

Suppression of monoclinic phase & vacancy concentration might be connected

Remnant Polarization

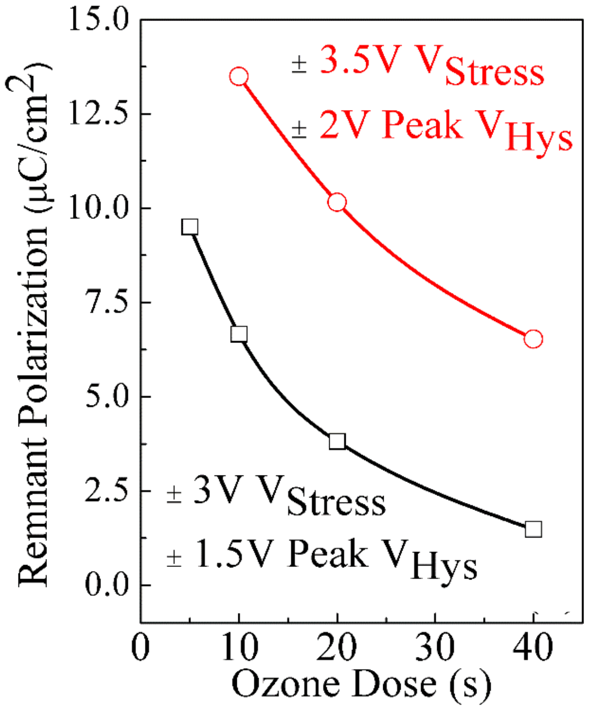

Lower O_3 Dose ⇒

- Lower monoclinic phase
- Higher remnant polarization
- Higher leakage current

A. Pal, et al., "Enhancing Ferroelectricity in Dopant-Free Hafnium Oxide", Applied Physics Letters 110, 022903 (2017)

IMI Results: Undoped FE HfO_2

- *In situ* XRD annealing study at SLAC reveals initial nucleation into tetragonal/orthorhombic phase followed by phase inversion to monoclinic phase during slow heating
- Likely a crystallite size/surface energy effect

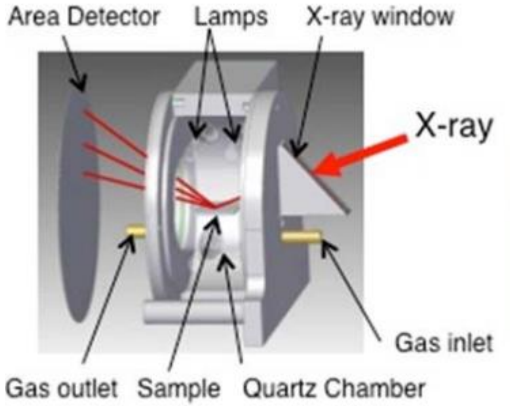

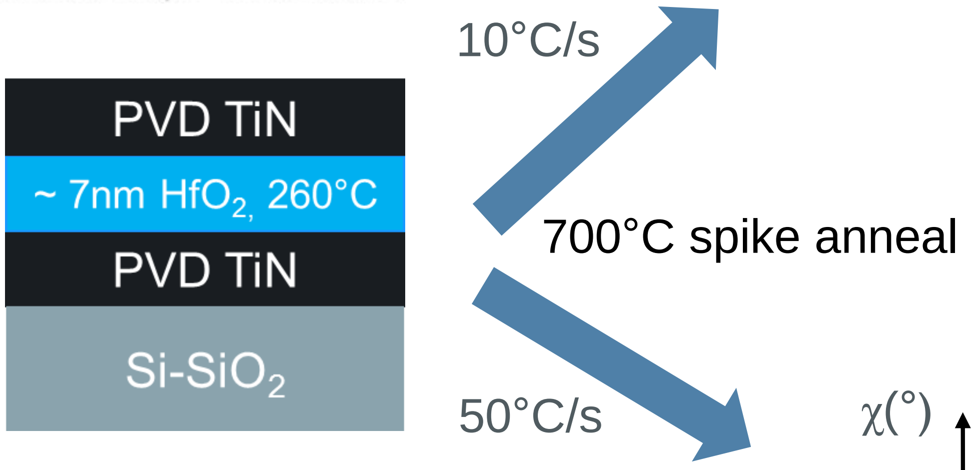

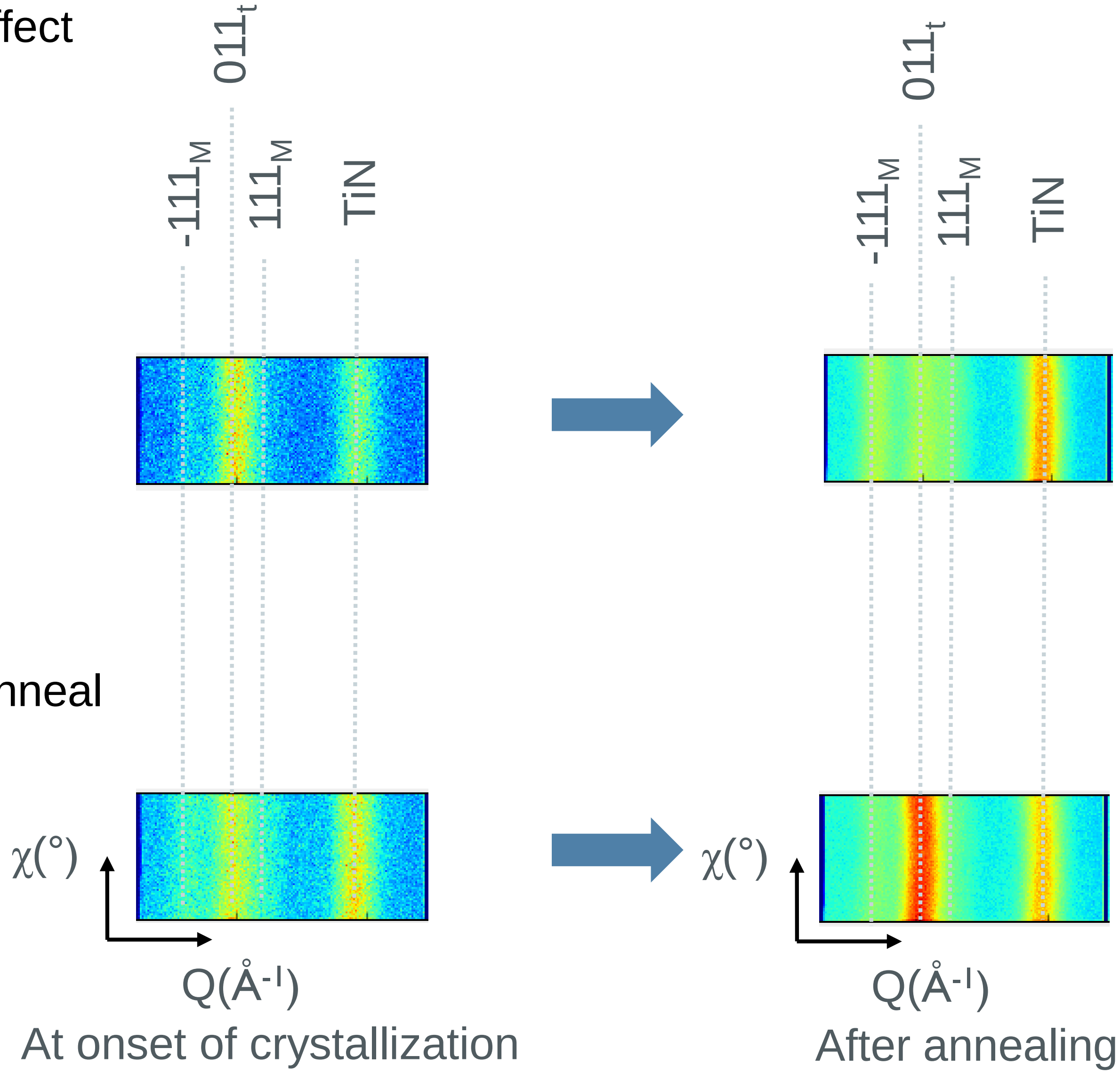

Narasimhan *et al.*, Unpublished Results

NVM Selectors

NVM Selectors: Sneak Current Elimination

Challenges with Sneak Current Paths for 3D Resistive Memory

Sneak current paths

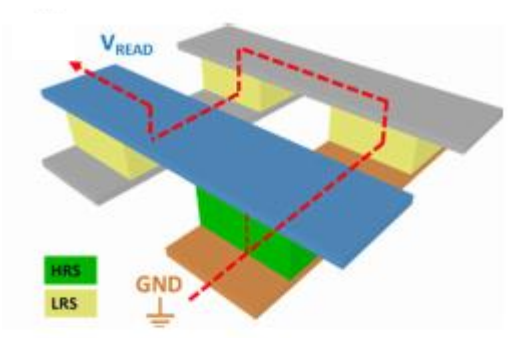

* Ref: Chen, et al. Journal of Electroceramics (2017): 1-18.

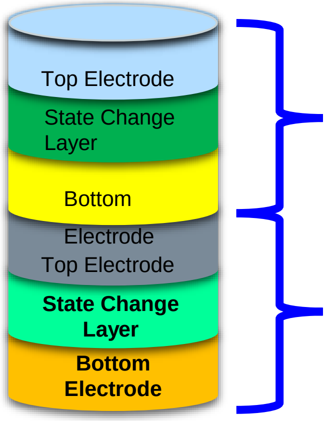

Memory Element
Eg: ReRAM, PCRAM, CBRAM

Selector Element
Eg: TMO, OTS, MSM, MIEC Diodes

Generic Two Terminal Memory Cell

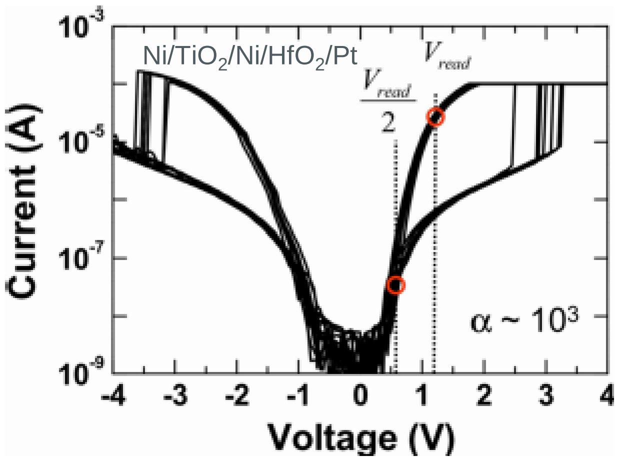

J.J. Huang, et al, IEEE Int. Electron Devices Meet. (2011), p. 31.7.1–31.7.4

- Selector devices are critical to eliminating sneak current paths
- Selectors needed to address performance, density and reliability requirements

Survey of NVM Selector Current Options

Type	MIEC	IMT	Tunnel barrier	FAST	OTS	Binary OTS
Material	Cu-based	NbO x	TaO /TiO /TaO	Unknown	AsTeGeSiN	SiTe
Source	IBM, 2012	POSTECH, 2015	POSTECH, 2014	Crossbar, 2014	SAIT, 2012	POSTECH, 2016
On. J [MA/cm^2]	0.08 (0.9 V)	4	>10 (2 V)	3	10	10
Off. J [kA/cm^2]	0.004	23	10	0.001	2	0.01
Selectivity	10^4	$>10^2$	10^2	$>10^6$	$>10^3$	10^6
SS [mV/dec]	100	<10	200	<5	<50	<1
Delay Time [ns]	50	?	20	30	20	10
Transition [ns]	15	<50	<20	5	5	2
Process T. [°C]	?	RT	300	300	?	RT

Ref: Chen, et al. Journal of Electroceramics (2017): 1-18.
Y. Koo, K. Baek, H. Hwang, In 2016 Symp. VLSI Technol. (2016)

MIEC: Mixed Ionic Electronic Conduction
IMT: Insulator Metal Transition
FAST: Field Assisted Superlinear Threshold selector
OTS: Ovonic Threshold Switch

- Choice of selector materials & devices in 3D implementation requires concurrent evaluation for performance, reliability, cost and ease of integration

NVM Selector Development

Material Understanding

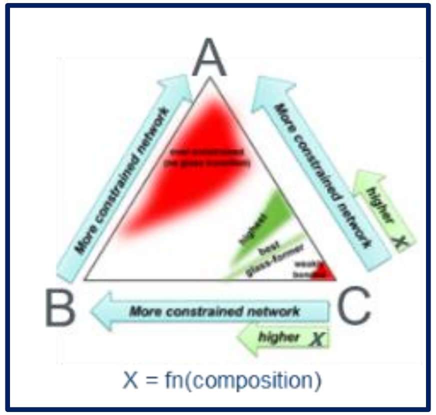

Define Compositional Space

Thermal Stability & Resistivity

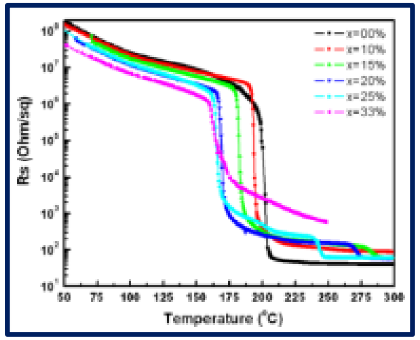

Screen Materials

Composition

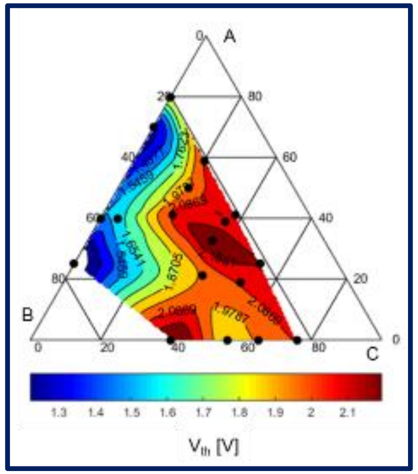

Select Promising Compositions

Parameters
Non-linearity
Threshold Voltage
Leakage (I_{off})
Switching time
Endurance

Electrical/ Reliability

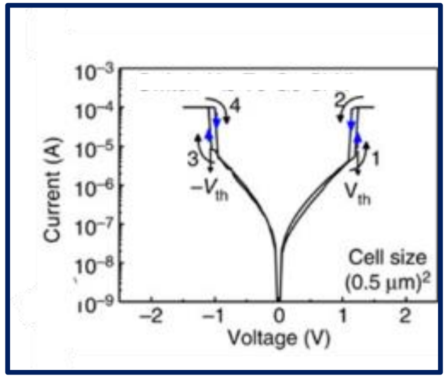

Converge on specs

IMI P-30 PVD Chamber

300mm Dep & Test

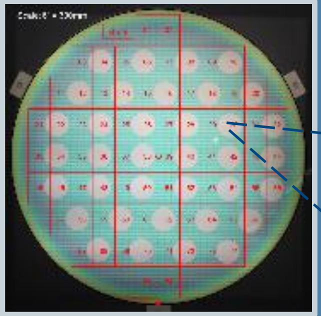

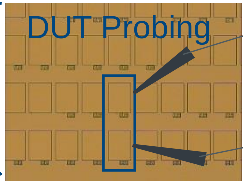

Successfully screened 1000's of OTS, MSM, MIEC and TMO compositions in 4 year period

Selector Materials Characterization

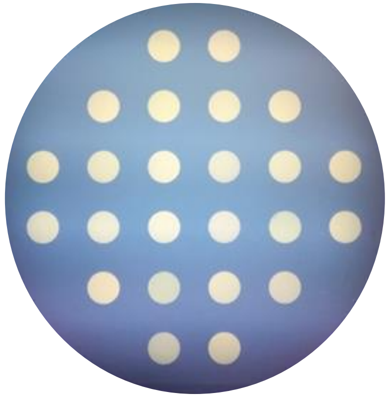

Physical Characterization

- Composition: XRF, XPS, EDX, RBS
- Resistivity: Resmap, R_s vs T
- Crystallinity: XRD, R vs T
- Roughness: AFM

Rs vs Temperature

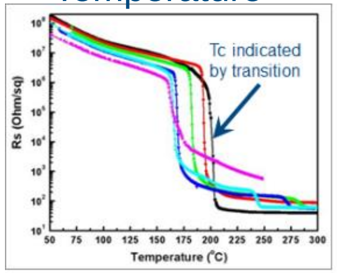

Tc vs Composition

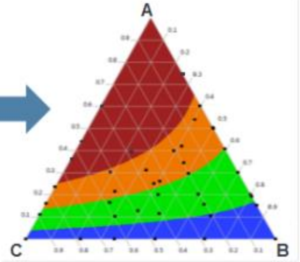

Electrical Characterization

Dep & Test Compatible Test-vehicle

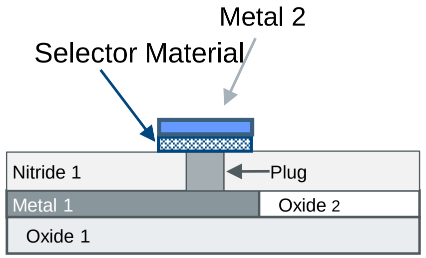

Level 1- DC IV
Fast Screening

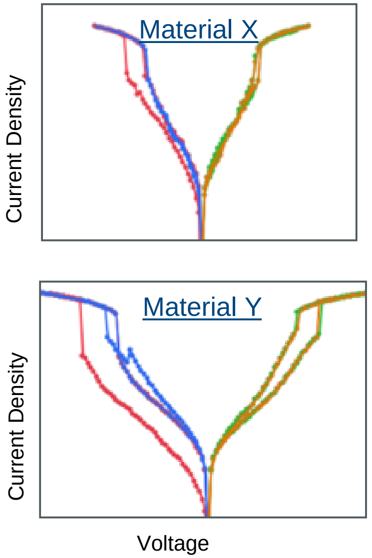

Level 2-Pulsed IV
Selected Splits

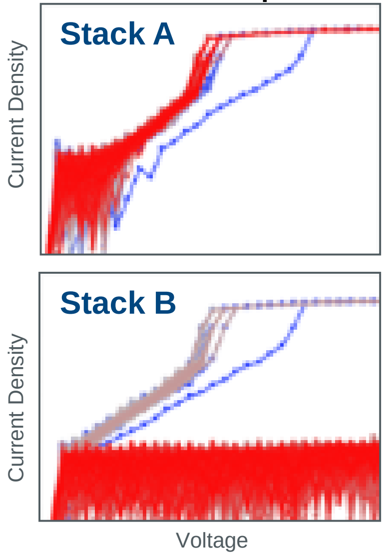

Level 3- Endurance
Champion Splits

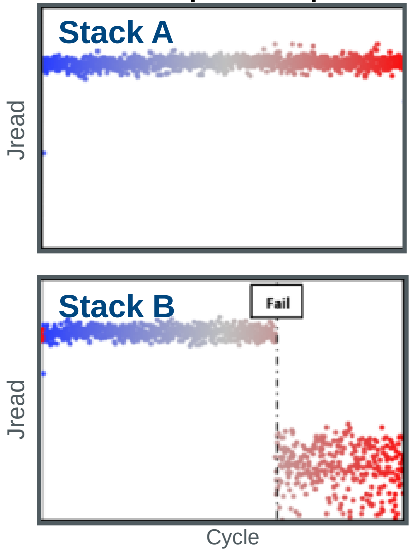

NVM Selector: 3D XPoint

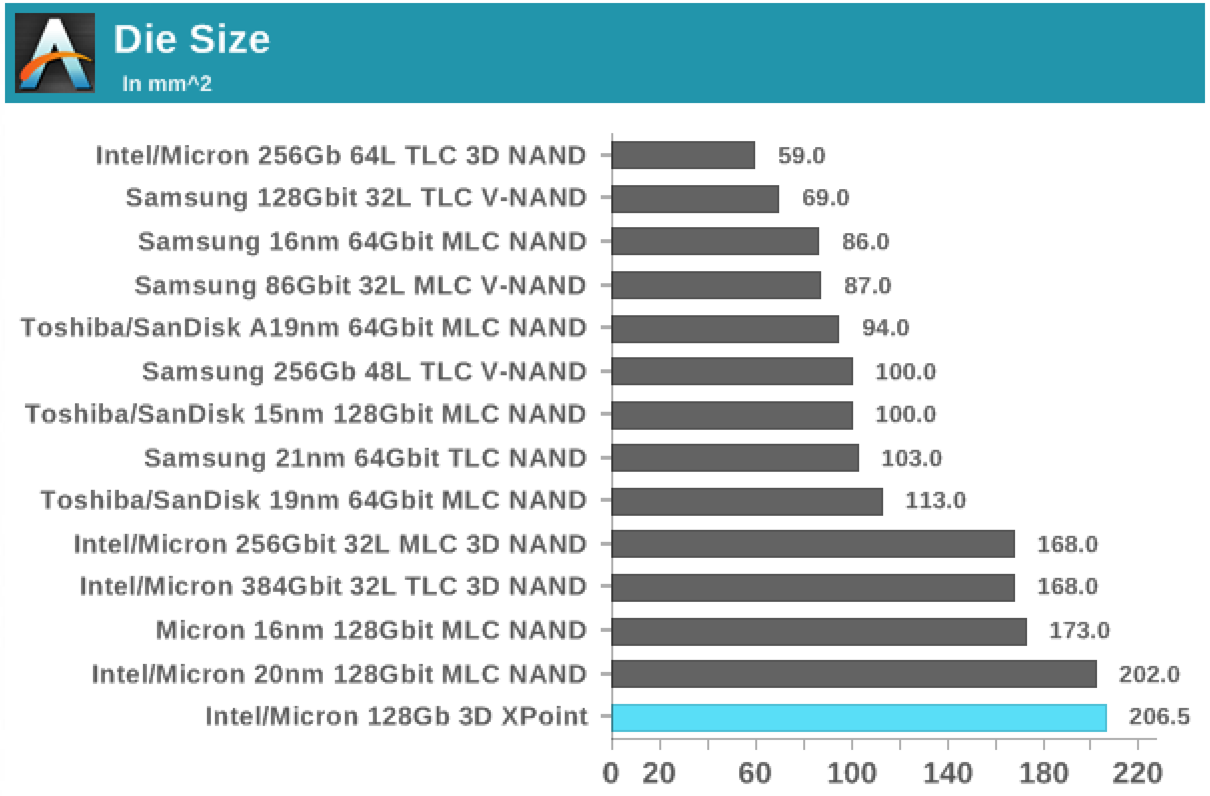

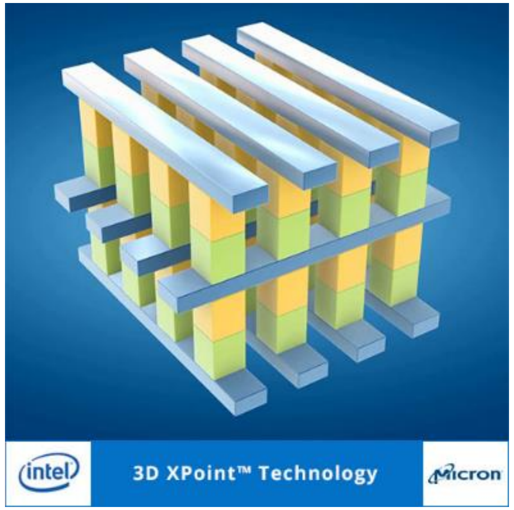

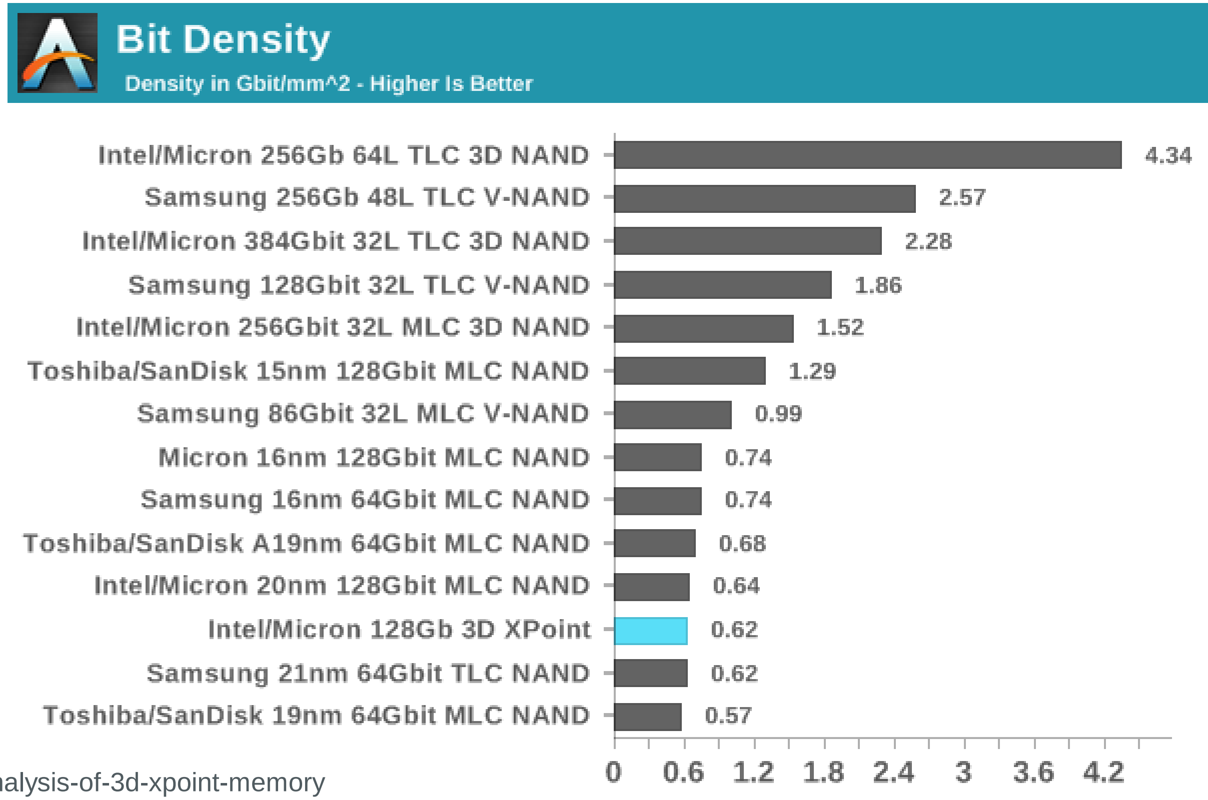

Size and density most similar to planar NAND

Critical litho for each layer may be cost disadvantaged vs. 3D NAND type flow with increasing layer counts

 Source: ANANDTECH http://www.anandtech.com/show/11454/techinsights-publishes-preliminary-analysis-of-3d-xpoint-memory

INTERMOLECULAR

3D Vertical NVM – Conformal Selectors:

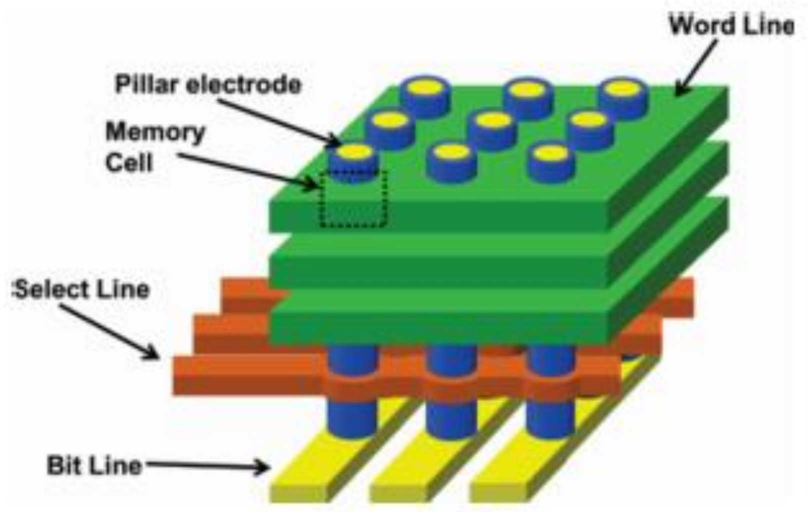

Y. Deng, et al, IEEE Int. Electron Devices Meet. (2013), p. 25.7.1–25.7.4.

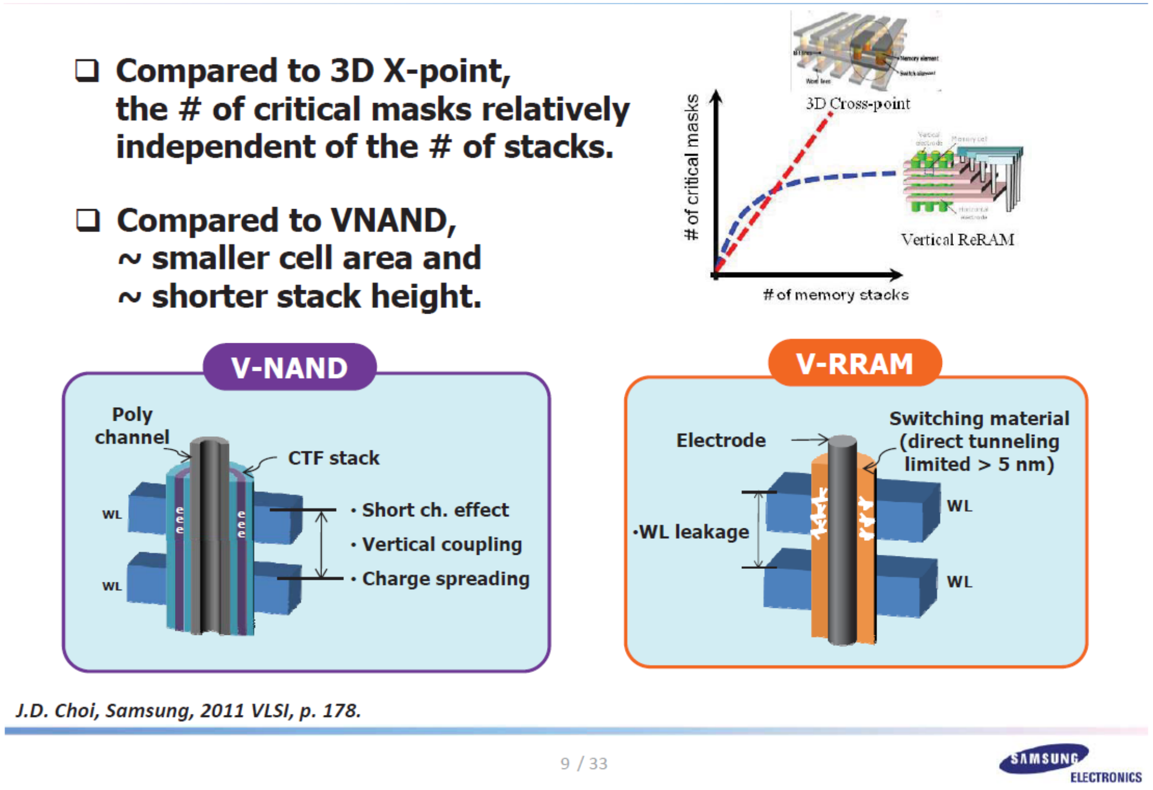

Need a conformal selector or self regulating cell (perhaps difficult to realize)

ALD Chalcogenides (ChG)

Key challenges

- Chalcogenides are used in advanced NVM applications
- 3D Vertical NVM architecture requires highly conformal deposition processes (e.g. ALD)
- Layered binaries require uniform composition and interface control
- ALD chalcogenide chemistry is complex and not well understood (i.e. not as simple as reactions with O_3 or NH_3)
- Elemental ALD is desirable to adjust stoichiometry of base system as memory/selector behavior is composition dependent
- Simplest chemistry is desired which also achieves performance requirements (e.g. stoichiometry, step coverage, thermal stability, electrical performance)

A-30 300mm ALD chamber with in-situ spectroscopic ellipsometry

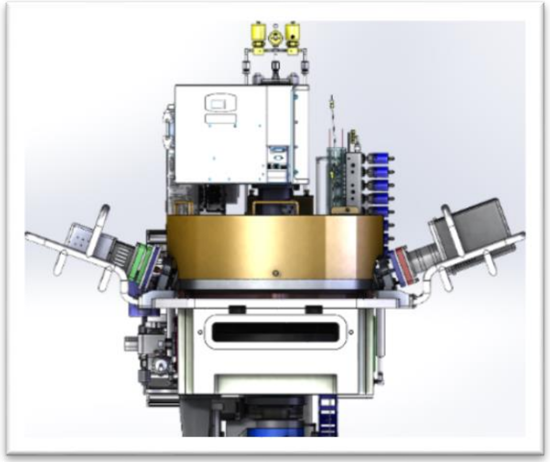

In-situ ALD Te growth monitoring on SiO2

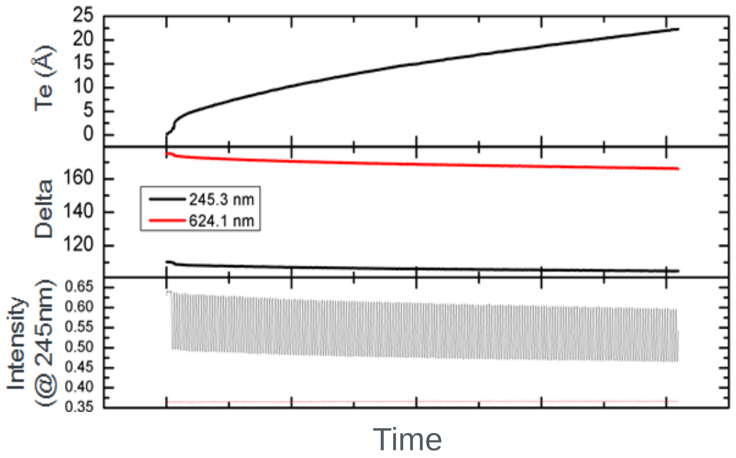

ALD Chalcogenide Selector Screening

Material Selection

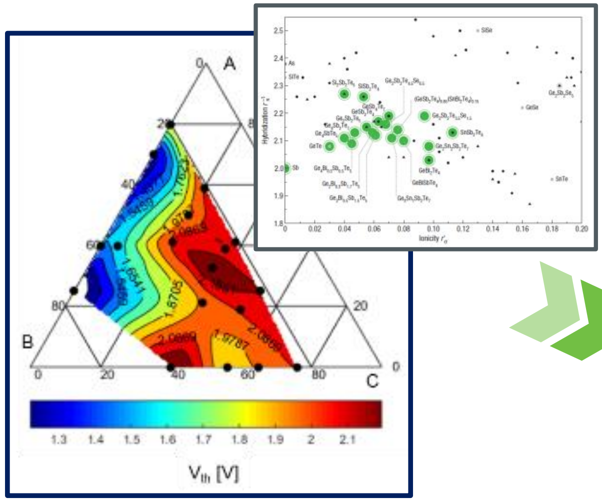

Select Promising Compositions (Leverage PVD Data/Modelling)

Process Development and Materials Characterization

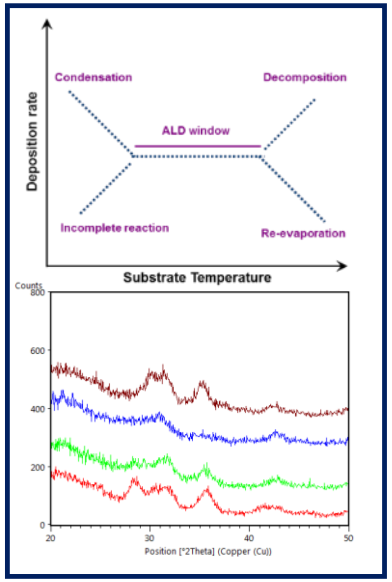

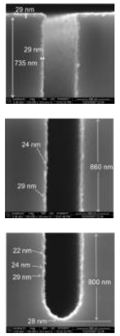

L(Se,Te) + R → (Se,Te) + RL ....etc.

Screen ligands/Develop ALD Unit Processes

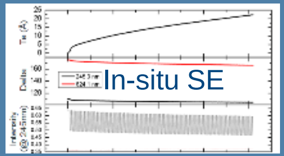

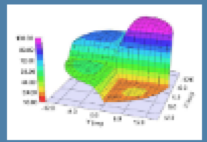

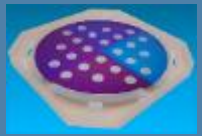

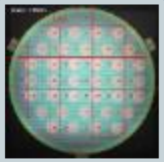

IMI A-30 ALD Chamber

Thermal Stability & Resistivity

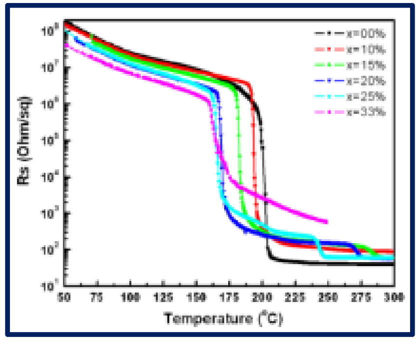

Test ALD Stacks and Nanolaminates

Parameter
Non-linearity
Threshold Voltage
Leakage (I_{off})
Switching time
Endurance

Electrical

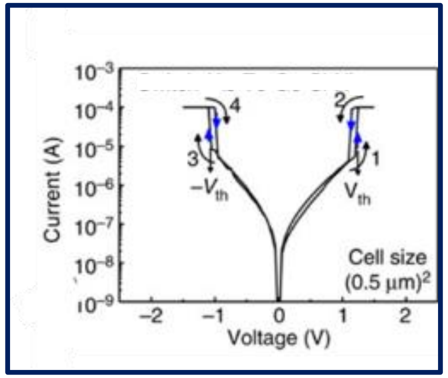

Electrical Response Feedback to Refine

ALD Chalcogenide (ChG) Approach

Example ALD ChG rxn pathways from literature to form binaries:

ALD GeS

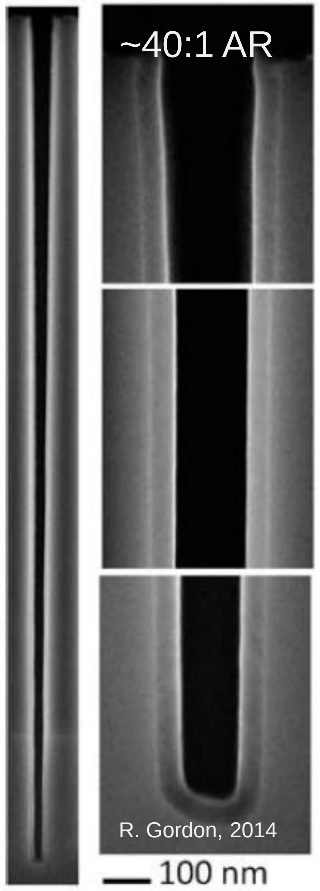

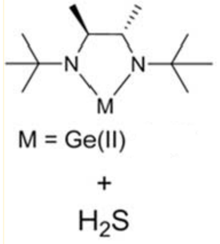

ALD GeTe

$(R_3Si)_2Te(g) + GeCl_2(g)$
$\rightarrow GeTe(s) + 2R_3SiCl(g)$

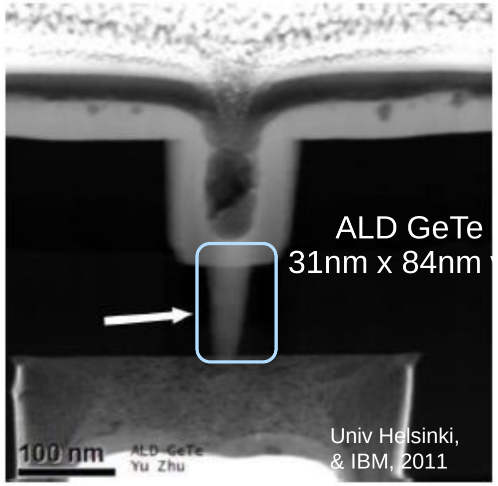

Example elemental ALD ChG under investigation at Intermolecular:

ALD Te

$(R_3Si)_2Te(g)$ + reactant screening

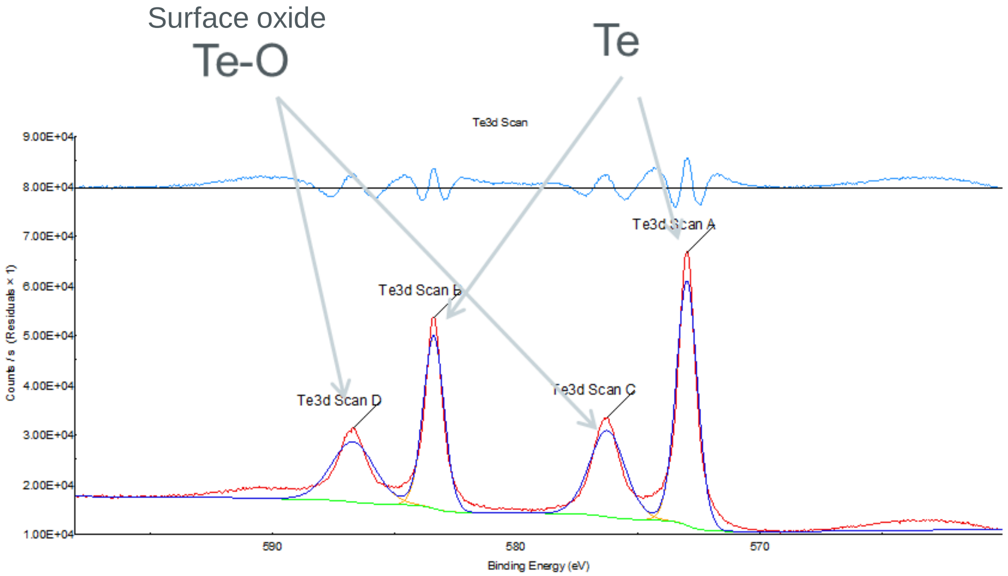

ALD Chalcogenide Selector Initial Results

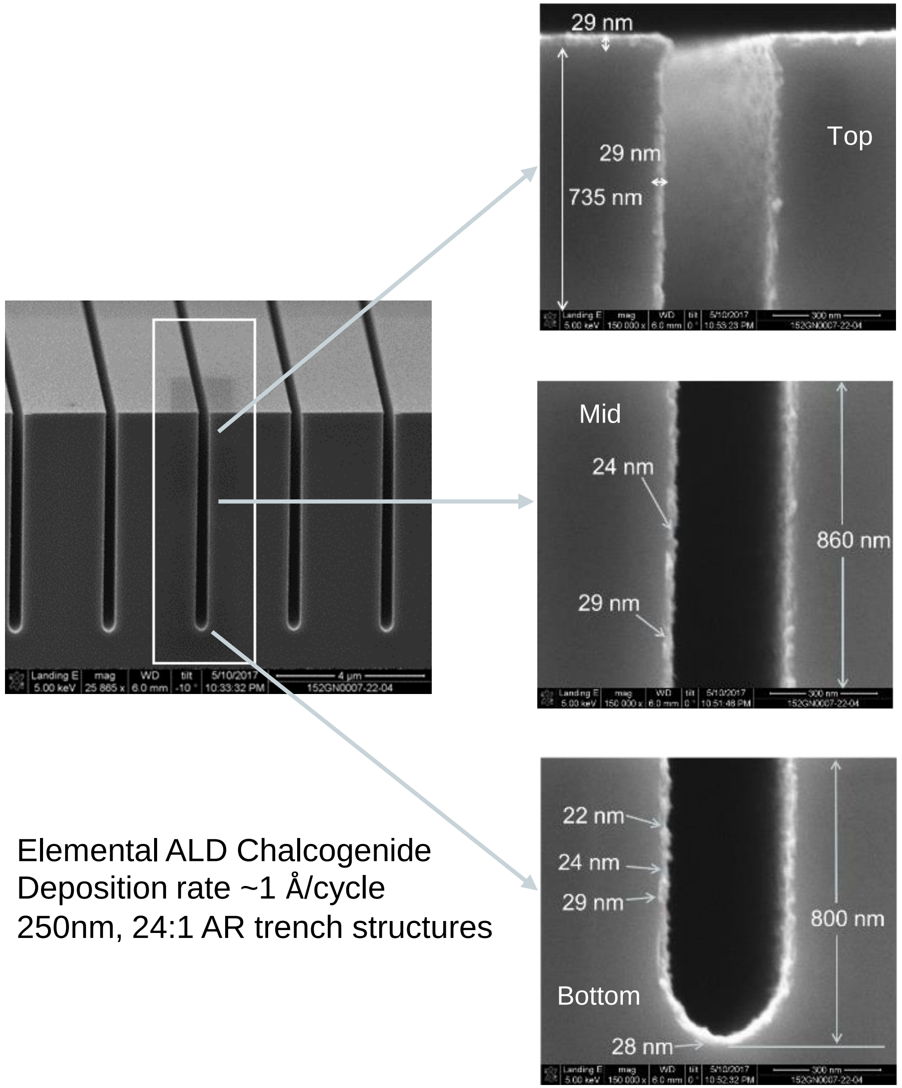

- Elemental ALD Chalcogenide
- Deposition rate ~1 Å/cycle
- 250nm, 24:1 AR trench structures

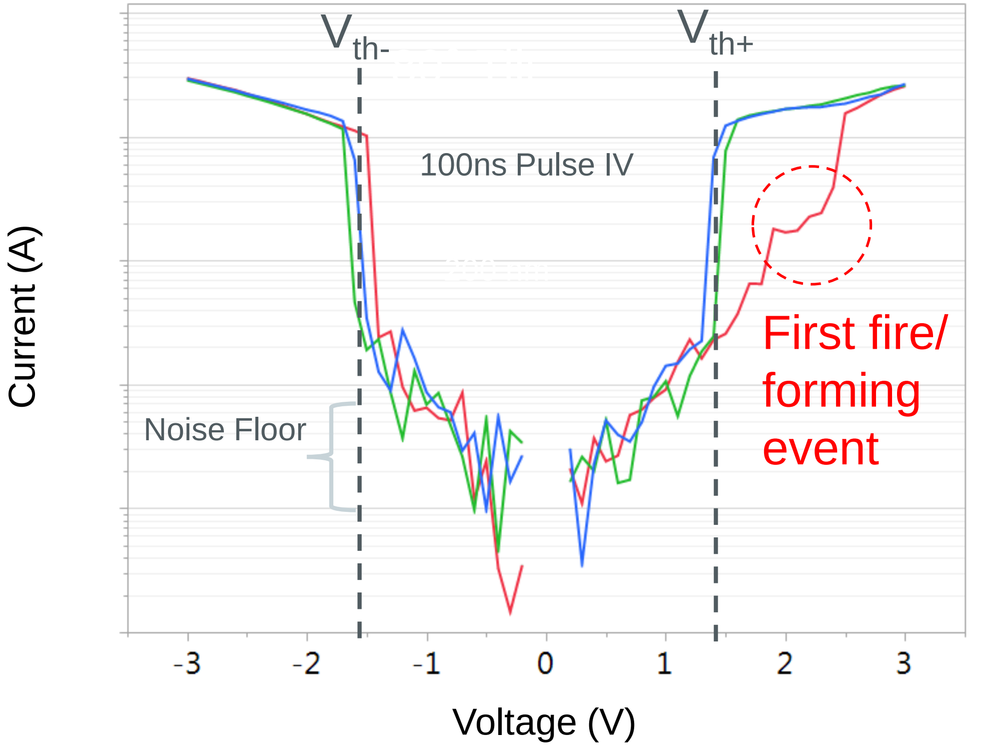

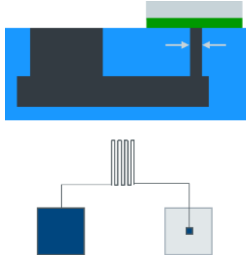

- ALD Chalcogenide Selector; elemental ALD to adjust composition of compound
- Conventional TiN Electrodes
- Pulse-mode electrical test (pulse width = 100 ns) shows clear, repeatable selector operation on 350 nm CD devices with forming event visible during first cycle
- Selector threshold voltage between 1.4-1.6V

ALD Chalcogenide Selector Initial Results

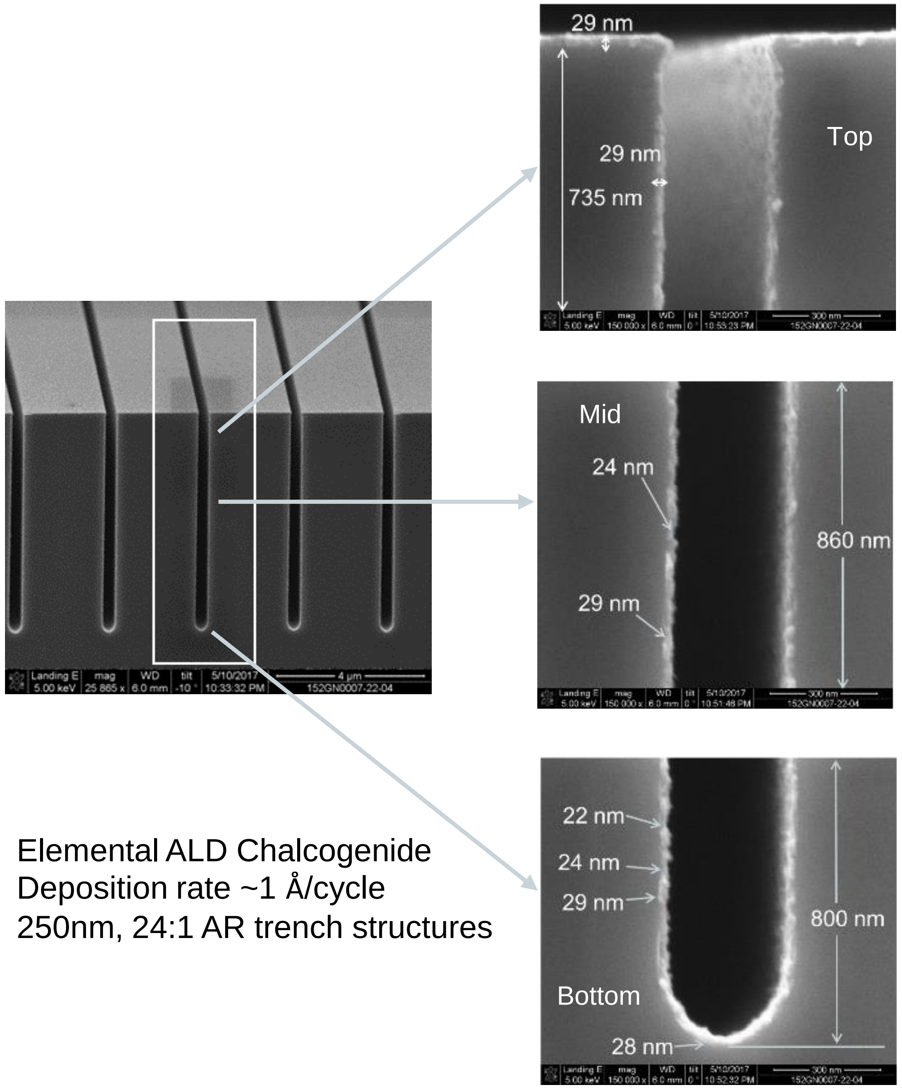

- Elemental ALD Chalcogenide
- Deposition rate ~1 Å/cycle
- 250nm, 24:1 AR trench structures

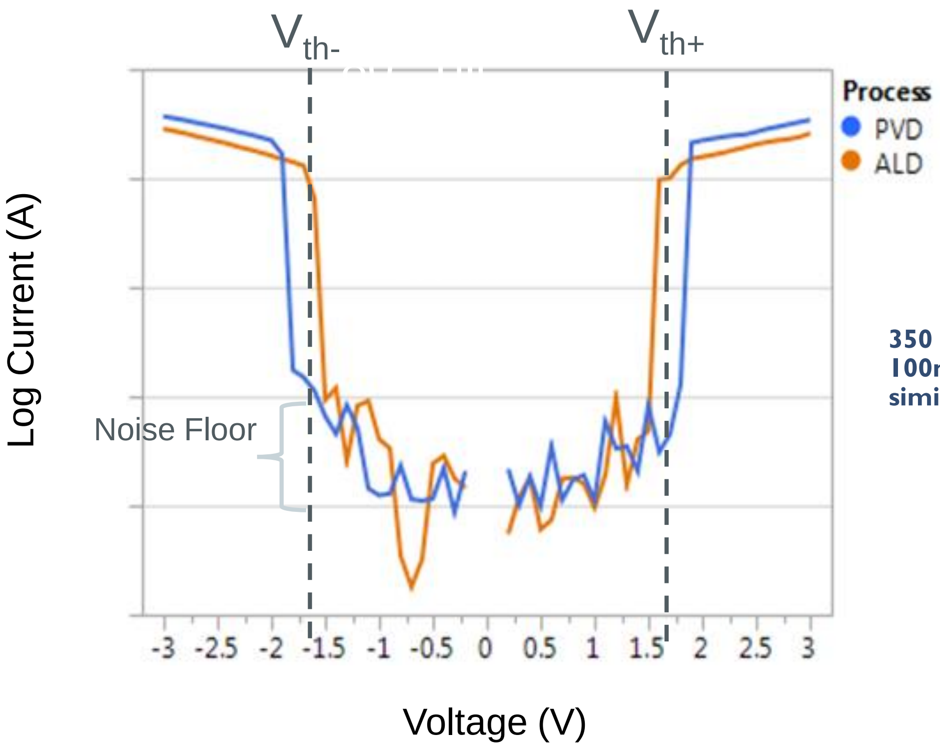

350 nm device size, 100ns Pulse IV, similar composition

- ALD Chalcogenide Selector; elemental ALD to adjust composition of compound
- Conventional TiN Electrodes
- Pulse-mode electrical test (pulse width = 100 ns) shows clear, repeatable selector operation on 350 nm CD devices with forming event visible during first cycle
- Selector threshold voltage between 1.4-1.6V

Summary

- Thin film HfO_2 based ferroelectric materials can enable advanced NVM and logic devices
- FE performance can be enhanced through stack design, composition tuning, and structure control
- 3D NVM architectures will require series connected non-linear selector elements
- A conformal selector with layer by layer compositional control can open up potential integration schemes and provide additional materials engineering control
- Initial feasibility using ALD Chalcogenide selectors with good conformality and similar electrical performance to PVD demonstrated

INTERMOLECULAR

Zr Rich Ferroelectric→ "Antiferroelectric Like" Transition

Bottom Electrode can be used to tune FE→AFE transition composition after field cycling

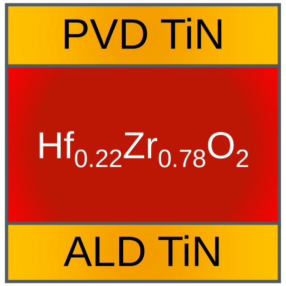

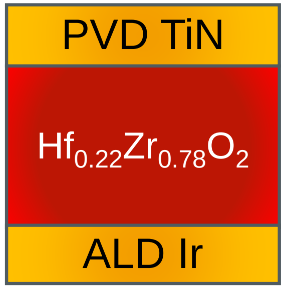

Before Wake-up After Wake-up

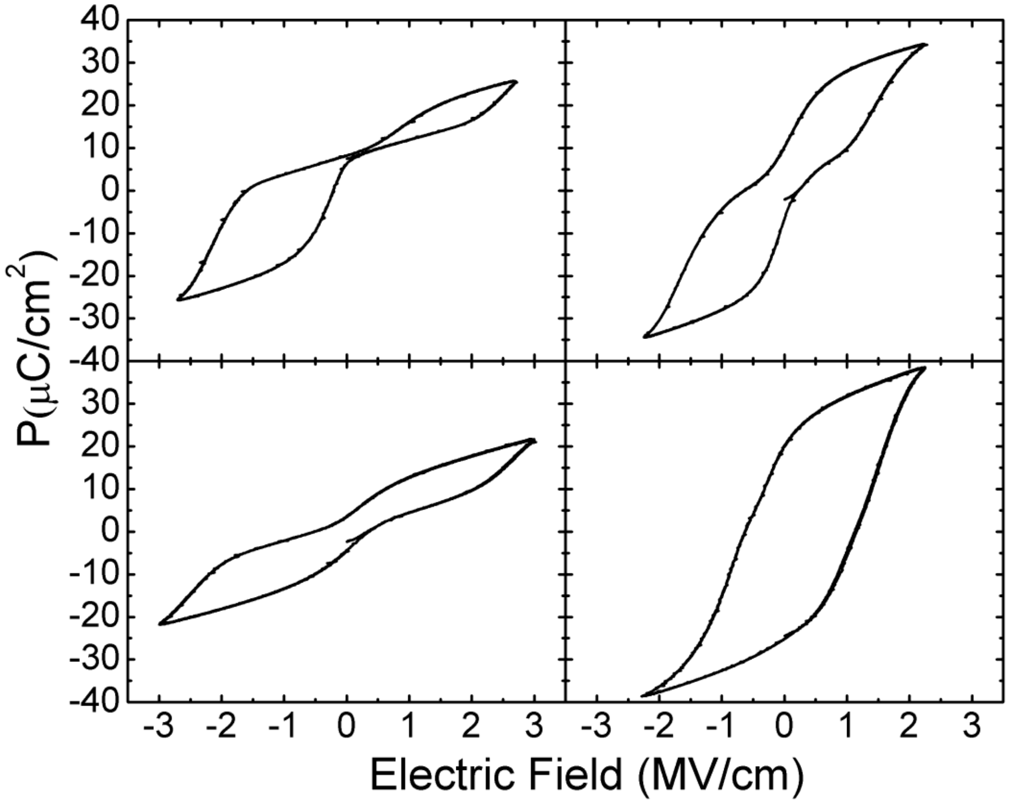

Pole Figure at 2θ=30° t/o (111)

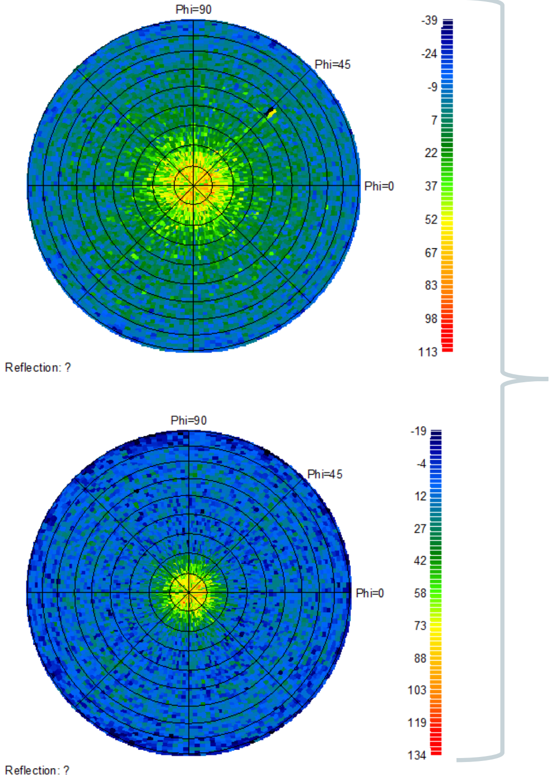

- Bottom electrode imparts some amount of texture
- Minimal impact on AFE vs FE response before wakeup

- Bottom electrode choice can enable ferroelectric response in more Zr rich solid solutions after "wake-up"

S. Weeks, et al., "Engineering of Ferroelectric HFO_2/ZrO_2 Nanolaminates", ACS Applied Materials & Interfaces (2017, submitted)

DFT Study of FE Switching Mechanism

- *Several* pathways exist with same low activation energy E_a, corresponding to *different* P_r values

Previously Reported Pathway

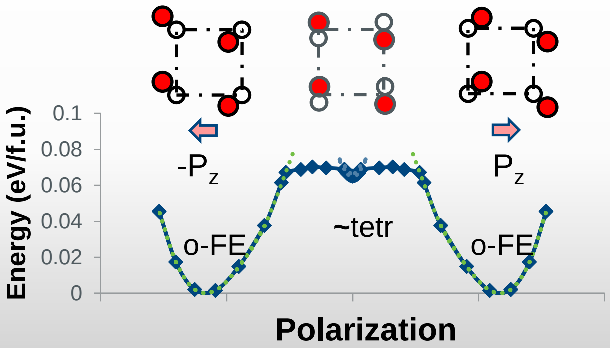

P=0.51 C/m^2 (HfO_2)
P=0.55 C/m^2 (ZrO_2)
$\Delta P = 2\ |\mathbf{P_z}|$

New Identified Pathways

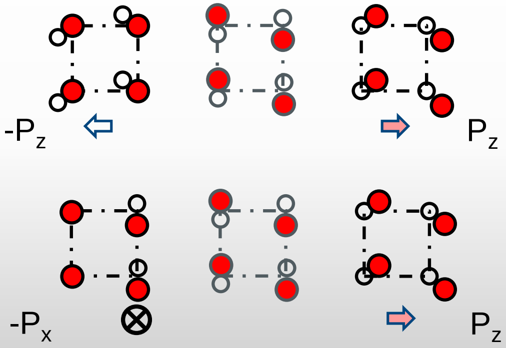

P=0.51 C/m^2 (HfO_2)
P=0.55 C/m^2 (ZrO_2)
$\Delta P = 2\ |\mathbf{P_z}|$

P=0.36 C/m^2 (HfO_2)
P=0.39 C/m^2 (ZrO_2)
$\Delta P = \sqrt{2}\ |\mathbf{P_z}|$

- P_r, E_c values likely sensitive to <u>domain wall energetics/kinetics</u> that would select one of the pathways
  - Strain, dopants, and/or deposition conditions may be potential knobs
- Preliminary calculations suggest that strain indeed strongly affects the preferred pathway => controls P_r, E_c

	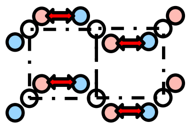	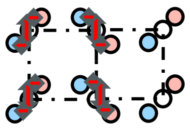	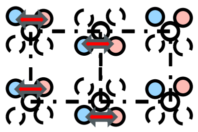	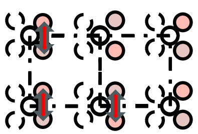	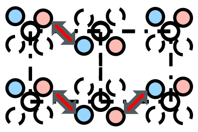
unstrained P	0.61C/m^2	0.55C/m^2	**0.55**C/m^2	0 C/m^2	0.61C/m^2
unstrained	0.18	0.19	**0.07**	0.19	0.3
tensile 5% ⊥ P	------------------ o-FE structure unstable ------------------				
compressive 5% ⊥ P	0.17	**0.06**	**0.07**	0.06	0.4
tensile 5% || P	0.2	0.08	**0.11**	0.19	0.19
compressive 5% || P	0.2	**0.12**	**0.12**	0.12	0.5

Activation energies (in eV/f.u.) for different switching pathways as indicated. Results in the presence of strain are preliminary (sparse NEB meshes).

S. Barabash, et al., "Ferroelectric Switching Pathways and Energetics in (Hf,Zr)O_2," ECS PRIME 2016, D02-1481

Selector Examples

MIEC

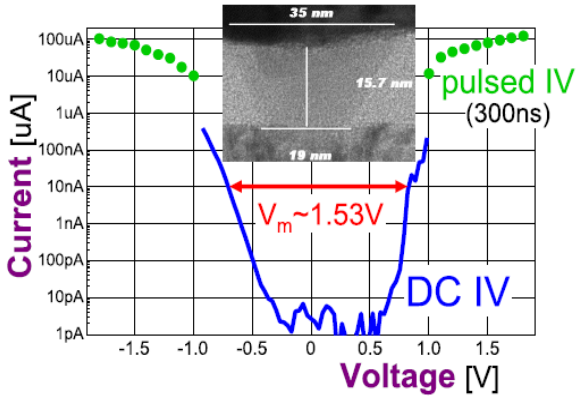

A. Padilla et al, TED15

FAST

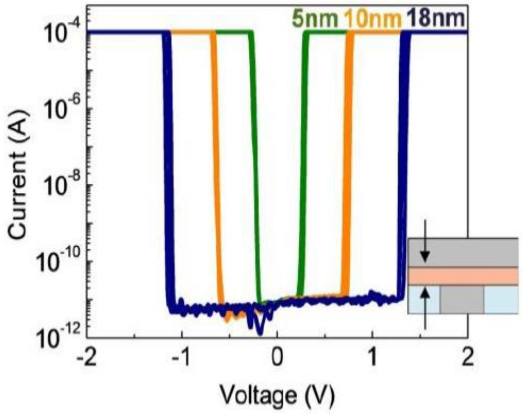

S. H. Jo et al, TED15

Chalcogenides

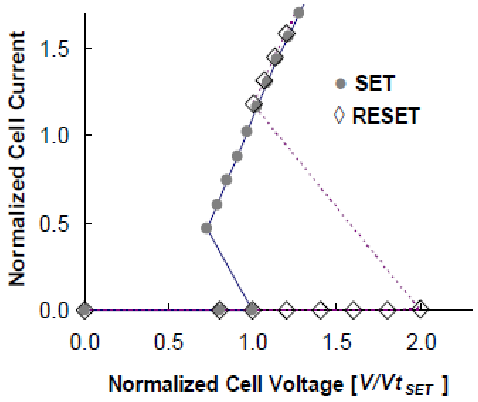

D. Kau et al, IEDM09

- Memory selector elements based on different material systems and physical mechanisms